Combined APSO-ANN and APSO-ANFIS models for prediction of pressure loss in air-water two-phase slug flow in a horizontal pipeline

Faezeh Moghaddas, Abdorreza Kabiri-Samani, Maryam Zekri and Hazi M. Azamathulla

ABSTRACT

Prediction of air-water two-phase flow frictional pressure loss in pressurized tunnels and pipelines is essentially in the design of proper hydraulic structures and pump systems. In the present study artificial neural networks (ANN) and adaptive neuro-fuzzy inference system (ANFIS) are employed to predict pressure loss in air-water two-phase slug flow. Adaptive particle swarm optimization (APSO) is also applied to optimize the results of the ANN and ANFIS models. To predict the pressure loss in two-phase flow, the frictional pressure loss coefficient needs to be determined with respect to the effective dimensionless parameters including two-phase flow Froude and Weber numbers and the air concentration. Laboratory test results are used to determine and validate the findings of this study. The performances of the ANN-APSO and ANFIS-APSO models are compared with those of the ANN and ANFIS models. Different comparison criteria are used to evaluate the performances of developed models, suggesting that all the models successfully determine the air-water two-phase slug flow pressure loss coefficient. However, the ANFIS-APSO performs better than other models. Good agreement is obtained between estimated and measured values, indicating that the APSO with a conjugated ANFIS model successfully estimates the air-water two-phase slug flow pressure loss coefficient as a complex hydraulic problem. Results suggest that the proposed models are more accurate compared to former empirical correlations in the literature.

Key words | air-water flow, APSO-ANFIS model, APSO-ANN model, pressure loss, slug flow, two phase flow

Faezeh Moghaddas
Abdorreza Kabiri-Samani (corresponding author)
Department of Civil Engineering,
Isfahan University of Technology,
Isfahan,
Iran
E-mail: *akabiri@iut.ac.ir*

Maryam Zekri
Department of Electrical and Computer Engineering,
Isfahan University of Technology,
Isfahan, 84156-83111,
Iran

Hazi M. Azamathulla
Department of Civil and Environmental Engineering,
University of the West Indies,
St. Augustine,
Trinidad and Tobago

HIGHLIGHTS

- ANN and ANFIS are employed to predict pressure loss in two-phase slug flow.
- APSO is also applied to optimize the results of the ANN and ANFIS models.
- Laboratory data are used to determine and validate the findings of this study.
- The performances of the ANN-APSO and ANFIS-APSO models are compared with those of the ANN and ANFIS models.
- The proposed models are more accurate than the former empirical correlations.

INTRODUCTION

Under exact circumstances, air may be supplied by vortices at water intakes, brought into the pressurized conduits, forming large bubbles in portions of the pipeline. Sequentially, the bubbles may result in an unstable two-phase flow, leading to severe periodic transient pressures inside the pipeline. Two-phase flow occurs when gas and

doi: 10.2166/hydro.2020.300

liquid co-subsist in a pressurized conduit. Slug, wavy, stratified, and stratified flows are some of the frequent two-phase flow regimes that are possible in pressurized conduits. Among these, slug flow is the most severe two-phase flow pattern that can lead to disruption of the systems operation (Mandhan *et al.* 1974). The joint effects of gas and liquid characteristics create a complex and periodic two-phase slug flow with different parameters engaged. Therefore, the study of air-water two-phase slug flow in hydraulic structures such as pressurized flow tunnels, inverted siphons, culverts and pressurized pipelines is of great importance for design purposes (Kabiri-Samani & Borghei 2010; Eyhavand-Koohzadi *et al.* 2016). In a pressurized two-phase flow, the pressure loss is governed by the complex mix flow behavior; i.e. losses due to sliding between the two phases at the interfaces. Accordingly, introducing an experimental friction coefficient for the mix air-water homogenous flow λ_{mix} into a conventional friction loss formula such as the Darcy–Weisbach is a rather general approach for estimating the pressure loss in a two-phase flow (Kabiri-Samani & Borghei 2010).

Investigation and control of flow phenomena in two-phase flow requires detailed knowledge of the two-phase flow pressure loss with respect to the phase properties. Two-phase flow pressure loss was primarily characterized based on the model experimentation methods that use flow visualization techniques or sensors. Numerous model experimentation-based techniques have been used to evaluate the pressure loss of two-phase flows (Lockhart & Martinelli 1949; Chisholm 1967; Muller & Heck 1986; Mishima & Hibiki 1996; Lee & Lee 2001; Kabiri-Samani & Borghei 2010; Zhang *et al.* 2010; Autee & Giri 2016; Kong *et al.* 2018; Dang *et al.* 2019; Lavin *et al.* 2019; Lewis & Wang 2019). Muller & Heck (1986) related pressure loss in the small diameter horizontal pipes (1–4 mm) to the mass quality, suggesting that pressure loss increases with the increase in mass quality. Kabiri-Samani & Borghei (2010) investigated the pressure fluctuations and pressure losses of air-water two-phase slug flow in a horizontal pipeline of 90 mm in diameter. They proposed a relationship for calculating the mixed air-water two-phase slug flow pressure loss coefficient. Autee & Giri (2016) investigated the two-phase flow pressure loss in small size channels of 4–8 mm in diameter. Kong *et al.* (2018) studied the effects of pipe size on two-phase flow regimes and pressure loss using the drift-flux model. Lavin *et al.* (2019) investigated the effects of rectangular channel inclination, whereas Dang *et al.* (2019) investigated the effect of circular pipe inner diameter on two-phase flow characteristics and pressure loss. However, these approaches often neither perform well nor exhibit accuracy, being often deficient in precision with certain drawbacks to accurately predict two-phase flow pressure loss. Therefore, computational intelligence approaches that avoid any subjective judgments, such as artificial neural networks (ANN) and supervised back-propagation (BP) (Sunde *et al.* 2005; Bara *et al.* 2013), self-organizing maps (Mi *et al.* 1998), an ensemble of competing feed-forward ANN (Mahvash & Ross 2008), probabilistic neural networks PNN (Timung & Mandal 2013), fuzzy logic inference systems (FLIS) (Le Corre *et al.* 1999), and adaptive neuro-fuzzy inference system (ANFIS) (Tsoukalas *et al.* 1997) can potentially overcome the disadvantages of classical methods.

Recently, soft-computing techniques such as ANN, FLIS and ANFIS have provided a powerful means for design and management purposes in hydraulic and environmental engineering (Zhang *et al.* 2006; Chen *et al.* 2008; Seckin 2010; Kabiri-Samani *et al.* 2011; Najafzadeh & Sattar 2015; Najafzadeh & Saberi-Movahed 2016; Najafzadeh & Shahid 2016; Lima *et al.* 2017; Najafzadeh & Bonakdari 2017; Najafzadeh 2019; Saberi-Movahed *et al.* 2020), and thus are widely used to solve complex phenomena such as two-phase flow problems including classification of two-phase flow regimes via image processing and a neuro-wavelet approach (Sunde *et al.* 2005), identification of two-phase flow patterns (Mahvash & Ross 2008), prediction of two-phase flow conditions over stepped chutes based on ANFIS (Hanbay *et al.* 2009) and calculation of volume fraction in stratified three-phase flow regime (Roshani *et al.* 2018). Among SC techniques, ANFIS, which is a hybrid intelligent scheme based on FLIS and ANN, forecasts outputs in uncertain situations and thus offers certain advantages for solving different hydraulic problems. Despite the capability of soft computing methods to solve complicated problems that conventional methods have not yet been able to solve, rather 'inexact' solutions with associated inaccuracies and uncertainties are inevitable (Sinha *et al.* 2000; Muleta & Nicklow 2002; Mousavi & Shourian 2009; McClymont *et al.* 2013; Shokouh Saljoughi *et al.* 2017; Ehteram *et al.* 2018; Thomas *et al.* 2019). Nevertheless, applications of

optimization algorithms such as particle swarm optimization (PSO), adaptive particle swarm optimization (APSO) and genetic algorithms (GA) (Azamathulla & Ahmad 2013) could effectively enhance the outcomes of SC-based methods and thus pave the way for investigating intrinsic complexities of the two-phase flows.

NOVELTY AND OBJECTIVES OF THE STUDY

Lack of a reliable means for predicting the frictional pressure loss in two-phase flow conduits hinders proper design of pressurized systems (Kabiri-Samani & Borghei 2010). There are several measurements with numerous liquid-gas combinations for different flow conditions. However, the correlations fitted to these data often hold a large number of constants and thus remain impractical. Furthermore, all the former regression and mechanistic methods still have very large deviations. Notably, due to the deforming interface of the liquid and gas, the exact shape and location of the regions occupied by each phase cannot be easily recognized, leading to an even more complicated situation. In the case of slug flow, there is an extra variation in dynamic pressure due to the changes in air pressure. Furthermore, most of the former investigations were performed on two-phase flow characteristics in small size channels, overlooking the complexities of two-phase flow in large size channels including hydraulic structures. To the authors' knowledge, limited information is available in the published literature on the hydrodynamic characteristics of air-water two-phase slug flow including pressure loss in hydraulic structures such as water tunnels and pipelines, inverted siphons and culverts. Therefore, implementation of a general and accurate approach for prediction of the two-phase slug flow pressure loss in water conduits is of great importance for design purposes.

This paper investigates the capabilities of ANN, ANN-APSO, ANFIS, and ANFIS-APSO in identifying air-water two-phase slug flow frictional pressure loss coefficient. The characteristic features of mechanistic two-phase slug flow model are selected as the ANN, ANN-APSO, ANFIS and ANFIS – APSO inputs. The performances of the models are assessed using the experimental datasets of Kabiri-Samani & Borghei (2010). APSO is employed to optimize fuzzy if–then rules of a gradient-based ANFIS model and thus prevent answers from local optimum entrapment. Therefore, the APSO algorithm enables optimization of ANN and ANFIS models configuration and adjustment of the antecedent and consequent parameters of fuzzy if–then rules by minimizing the error values. Finally, sensitivity analysis of the involved variables and discussions on the developed models are provided.

METHODOLOGIES AND MODELS

ANN

A conceptual arrangement of an ANN model employed in the present study is illustrated in Figure 1 (Sinha *et al.* 2000). This configuration analogizes a multi-layer perceptron model primarily fed by a dataset ($x_1, x_2, \ldots, x_n$) via the input layer to produce an expected result y in the output layer. The number of nodes in each layer is assessed by a trial-and-error procedure. Multiplying every input by its interconnection weight, summation of the product and then passing the sum via a sigmoid transfer function are the major processes undertaken by each node to produce its result. The back propagation (BP) algorithm is used to train ANNs (Rumelhart *et al.* 1986). Figure 2 illustrates a schematic configuration of a common radial basis function (RBF) network with n, l and m nodes in the input, hidden, and output layers, respectively (Sinha *et al.* 2000).

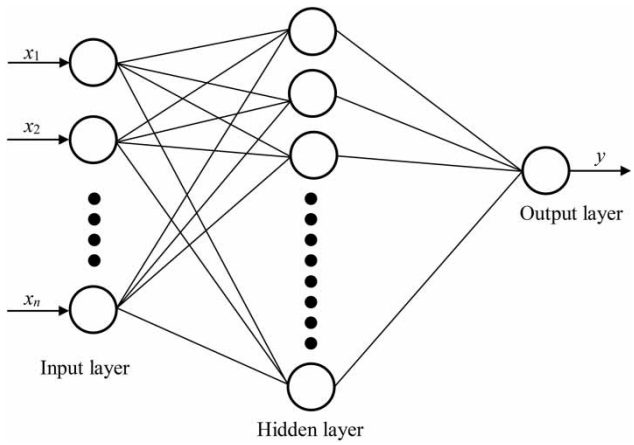

Figure 1 | Structure of a typical ANN model (Sinha *et al.* 2000).

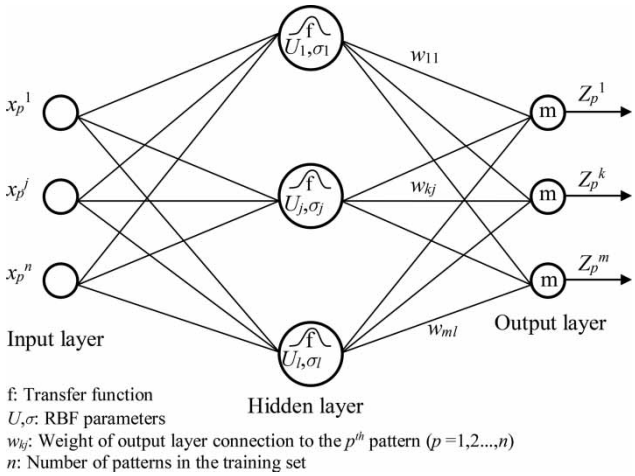

Figure 2 | Structure of a radial basis function (Sinha *et al.* 2000).

To optimize the parameters of the RBFs, we applied the minimum description length algorithm proposed in Leonardis & Bischof (1998). On the basis of trial-and-error procedure among different trained models, an ANN model with three layers and three, eight, and one neuron in the input, hidden, and output layers, respectively, provides the best results with the minimum least square error.

ANFIS

This section introduces the architecture of an ANFIS model. Figure 3 depicts a schematic architecture of a fuzzy inference system (FIS) model with two fuzzy if–then rules, two inputs x_1 and x_2 and one output y in a Takagi–Sugeno–Kang (TSK) form fuzzy rule base (Jang 1993). The FIS model contains five layers with respect to its conjunction with tuning algorithms (Figure 3). Membership functions of input variables are defined in Layer 1. Briefly, an FIS model comprises the following steps:

$$O_i^1 = \sigma_{Ai}(x) \tag{1}$$

$$w_i = \sigma_{Ai}(x) \times \sigma_{Bi}(x), \qquad i = 1, 2. \tag{2}$$

$$\bar{w} = \frac{w_i}{w_1 + w_2} \qquad i = 1, 2. \tag{3}$$

$$O_i^4 = \bar{w}_i f_i = \bar{w}_i (p_i x + q_i y + r_i) \tag{4}$$

where A_i is the linguistic variable, x is the input to node i, and O_i^1 is the membership of A_i, w_i represents the firing strength of the rule and p_i, q_i, r_i are the parameters of the consequent part of the rule i.

Finally, layer 5 with only one node simply sums all the outputs that come from layer 4 (Zanganeh *et al.* 2011).

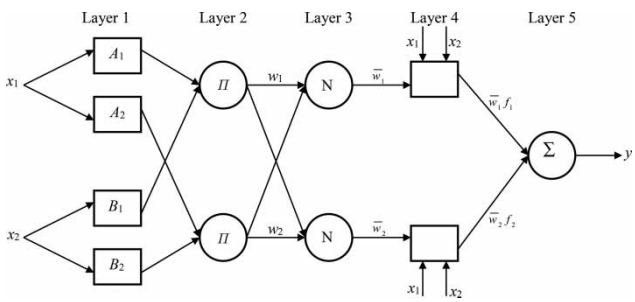

Figure 3 | Schematic of the structure of an ANFIS model (Sinha *et al.* 2000).

Subtractive clustering method

In this paper, the fuzzy if–then rules are extracted, applying a subtractive clustering approach in which the number and structure of fuzzy rules are adjusted by clustering parameters, implementing the following steps:

i. finding the data with the greatest potential to be the first center;
ii. separating all the data adjacent to the first center by a specified radius;
iii. repeating these steps to specify all the other clusters.

Cluster center for a set of k data is determined via the potential value of each data point as:

$$P_{ok} = \sum_{j=1}^{k} \exp\left(-4\sqrt{\sum_{i=1}^{n}\left(\frac{z_k^i - z_j^i}{ra_i}\right)^2}\right) \tag{5}$$

where P_{ok} is the potential of the kth data point, ra_i is the cluster radius of the ith dimension of the point, and z_k^i is the ith-dimensional data point (Chiu 1994). The first cluster center is considered as the point with the maximum potential.

PSO algorithm

Kennedy & Eberhart (1995) first developed the PSO evolutionary computation algorithm. The PSO algorithm's exploration is based on tracing each particle's best position in its history, P_b, and all particles' best position in their history, P_g, to arrive quickly around the global optimum. Considering $X_i = (x_{i1}, x_{i2}, \ldots, x_{iD})$, $V_i = (v_{i1}, v_{i2}, \ldots, v_{iD})$, $P_{ib} = (p_{i1}, p_{i2}, \ldots, p_{iD})$ and $P_g = (p_{g1}, p_{g2}, \ldots, p_{gD})$ as the current location and the velocity of the ith particle, the best position of the ith particle searching until now and the best position of the total particle swarm searching until now, respectively (where D is the dimension of the searching space and n is the total number of particles), the original PSO algorithm is expressed as (Kennedy & Eberhart 1995):

$$v_{id}(t+1) = v_{id}(t) + ac_1 \times rand() \times [p_{id}(t) - x_{id}(t)] + ac_2 \times rand() \times [p_{gd}(t) - x_{id}(t)] \quad (6a)$$

$$x_{id}(t+1) = x_{id}(t) + v_{id}(t+1) \quad 1 \le i \le n, \quad 1 \le d \le D \quad (6b)$$

where ac_1, ac_2 are constants with positive values ($ac_1 + ac_2 \le 4$, (Carlisle & Dozier 2001), rand() is a random number in the range of [0, 1] and $v_{id} \in [v_{\min}, v_{\max}]$. The performance of the PSO algorithm can be improved significantly by introducing inertial weights w into the previous PSO algorithm creating an adaptive PSO (APSO) algorithm (Shi & Eberhart 1998). After properly modulating the parameters w and $v_{\max}$ for the APSO algorithm, the convergence rate is increased; thereby the ability to search the global optimistic result is improved. APSO can be expressed as:

$$v_{id}(t+1) = w \times v_{id}(t) + ac_1 \times rand() \times [p_{id}(t) - x_{id}(t)] + ac_2 \times rand() \times [p_{gd}(t) - x_{id}(t)] \quad (7a)$$

$$x_{id}(t+1) = x_{id}(t) + v_{id}(t+1) \quad 1 \le i \le n, \quad 1 \le d \le D \quad (7b)$$

As the generation increases, the algorithm can progressively reduce w by tuning its value. After each generation, the worst particle is substituted by the best particle in the last generation, yielding a better result. Since the searching space and thereby the step length for the parameter w reduce step by step nonlinearly, the APSO algorithm is more effective compared to the PSO algorithm (Azamathulla & Ahmad 2013).

In the early stages of the algorithm, w should be reduced rapidly, whereas around the optimum it should be reduced slowly. Therefore, the following selection approach was adopted:

$$w = \begin{cases} w_{\max} - \left(\dfrac{w_{\min}}{\max gen1}\right) \times gen, & 1 \le gen \le \max gen1 \\ (w_{\max} - w_{\min}) \times e^{\left(\dfrac{\max gen1 - gen}{k}\right)}, & \max gen1 \le gen \le \max gen2 \end{cases} \quad (8)$$

where $w_{\min}$ is the initial inertial weight, $w_{\max}$ is the inertial weight of the linear section ending, max $gen2$ is the total searching generation, max $gen1$ is the used generations in which inertial weight is reduced linearly, and gen is a variable whose range is [1, max $gen2$]. By adjusting k, different final values of w are obtained. The APSO model begins with a collection of randomly generated solutions and then updates the swarm by using Equations (7a) and (7b) in each iteration. This procedure is continued until the stopping conditions are met. The stopping criteria require a fixed answer for some subsequent iteration; a minimized normalized root mean square error (NRMSE) of the estimations is then obtained as the objective function of the APSO optimizer:

$$NRMSE = \frac{1}{N}\sqrt{\frac{\sum_{i=1}^{n}(O_i - P_i)^2}{\sum_{i=1}^{N}(P_i - \bar{P})^2}} \quad (9)$$

where N is the number of data, O_i and P_i are the estimated and observed (target) values, and $\bar{P}$ is the average of the observed data. Figure 4 shows the variation of w with the number of generation.

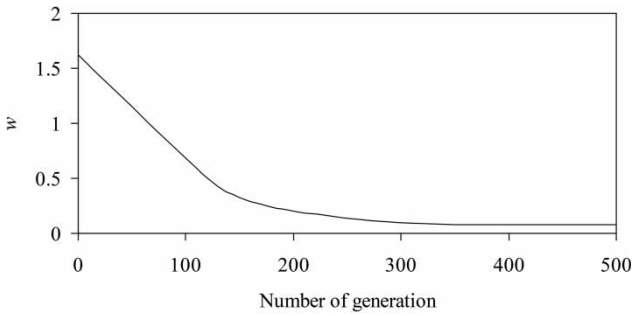

Figure 4 | The reduction scheme for value of the inertia weight.

PROPOSED METHODS

Combined ANN and APSO

The ANN–APSO hybrid algorithm is applied in this study by combining the APSO algorithm with RBF in which the search for the optimum starts by utilizing the APSO, thereby the training process is expedited (Figure 5(a)). While the value of fitness function is not amended for some generations or the alteration may become very small, the searching progress is switched to gradient descending search. The ANN–APSO algorithm's searching criteria include: (i) initializing a group of random particles, (ii) updating all particles according to Equations (6a) and (6b) until a new set of particles are generated, (iii) employing those new particles to find the global best position, and (iv) applying the BP algorithm to search around the global optimum. The stages of this hybrid algorithm are summarized below:

(i) Initializing randomly the positions and velocities of a group of particles, ranging from 0 to 1; (ii) Evaluating each particle's fitness value; (iii) If the maximal iterative generations are reached, then Step (viii) is performed; otherwise, Step (iv) is performed; (iv) Storing the best particle of the recent particles, updating the positions and velocities of all particles (Equations 7(a) and 7(b)) and generating a group of new particles; (v) Evaluating each new particle's fitness value and restoring the worst particle by the best particle; (vi) Reducing the inertial weights w according to Equation (8); (vii) If the existing P_g is fixed for the considered generations, then Step (viii) is performed; otherwise, Step (iii) is performed; (viii) Employing the BP algorithm to search around P_g for various epochs. If the search result is better than P_g, then the current search result is the output; otherwise, P_g is the output. The parameter w in the above ANN–APSO algorithm also reduces progressively by increasing iterative generation. The parameter max $gen1$ is generally adjusted by a trial-and-error procedure and then an adaptive gradient descending method is applied to search around the global optimum P_g.

Combined ANFIS and APSO

In the ANFIS–APSO model, the weights of the fuzzy antecedent parameters and the consequent parameters in the fuzzy rule-based system are adjusted through the APSO learning algorithm that searches for the optimal clustering parameters (Figure 5(b)). This model enhances the searching

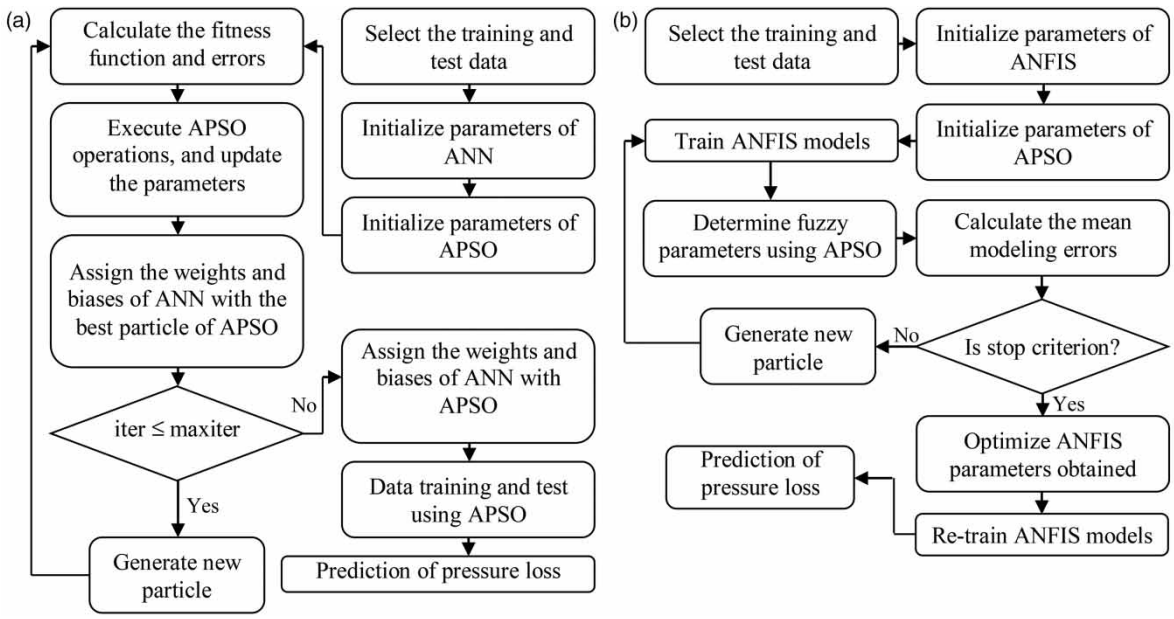

Figure 5 | The process of optimizing in: (a) ANN-APSO hybrid algorithm parameters and (b) ANFIS-APSO model parameters.

ability and implementation of ANFIS model to solve complex nonlinear problems such as pressure loss in a two-phase flow. Obtaining the best cluster parameters in the ANFIS–APSO model is a time-consuming trial-and-error procedure, particularly when numerous influential variables are involved. Hence, the fuzzy antecedent and consequent parameters are optimized by applying the normalized root mean square error (NRMSE) to improve the performance of the ANFIS–APSO model. In addition, ANN applies the mean squared error (MSE) to tune the FIS parameters. While developing the ANFIS–APSO model, different learning algorithms with different epochs were tested to define a model that has the best potential estimation ability for the prediction of observed results. The best correlation was then found through a hybrid learning algorithm and 1,000 epochs. Two different program codes were developed using MATLAB 8.0.1.604 software for the ANFIS and ANN simulations (MathWorks R2007b 2007).

EXPERIMENTAL MODEL, DATA, AND IMPORTANT VARIABLES

Experiments were conducted in a horizontal air-water flow pipeline at the hydraulic laboratory of Sharif University of Technology, Iran (Kabiri-Samani & Borghei 2010). It included a 10 m long transparent pipe with an inner diameter of 90 mm, a closed water circuit, an open air circuit, and test sections. The air-water mixture was allowed to flow in the two-phase flow section over a distance of 40 times the pipe diameter before entering the measurement section. The entrained air was released directly into the atmosphere at the end of the main pipe from the downstream reservoir. The frictional pressure loss, excluding the static pressure loss, for inclined flow direction was measured using variable reluctance differential dynamic pressure transducers (VDPT). The pressure sensors were variable reluctance differential pressure transducers that measured pressure from 88 to 350 cm of the water column at a frequency of 100 Hz. For the purpose of this study, the data acquisition system was used to measure transient pressures in different situations simultaneously. In order to exclude the influent effect on the flow, the first point for pressure loss measurement was selected at 4.02 m from the pipe inlet, which is much more than the required length as suggested for single- and two-phase flows (Woods *et al.* 2006; Kabiri-Samani & Borghei 2010). The locations of VDPTs for measurement of two-phase flow pressure were 4.02, 5.22, 7.12 and 8.92 m from the upper reservoir. The air/water rate ratios were between 0.04 and 2. A PC with a data acquisition system used to record the data, and digital cameras were employed to visualize the flow behavior. Digital cameras and scales were also used for measuring the air-water interface profile, slug flow wave length, and void fraction. Notably, since a transient pulsating pressure occurred, the time-averaged pressure was employed to determine the pressure losses of a steady state two-phase slug flow between different longitudinal sections. Sensitivity analysis inferred that a recording time of 150 seconds is the optimum for all the variable test requirements, including extreme values (Kabiri-Samani *et al.* 2007). Notably, most of the former investigations were performed on two-phase flow characteristics in small size channels, overlooking the complexities of two-phase flow in large size channels including hydraulic structures. Furthermore, most studies have been carried out on liquids other than water, such as oil, which is mostly used in chemical engineering. Therefore, we just applied the data of Kabiri-Samani & Borghei (2010). Overall, from a total of 210 tests, 1,260 measured data of pressure loss, covering all the two-phase slug flow hydraulic/geometric conditions, were employed in the present modeling.

There are two common phenomenological models for gas/liquid two-phase flows including homogenous and separate two-phase flows. A homogeneous fluid flow is a convenient concept for modeling two-phase flow pressure loss; it is a pseudo-fluid that complies with the conventional design equations for single-phase flow. Therefore, the fluid is characterized by suitably averaged properties of the liquid and gas phases. Considering the forces acting to the flow and according to the former experimental studies and the existing empirical correlations, from a physical viewpoint the relation between the dominant dimensional input and output parameters can be written as (Kabiri-Samani & Borghei 2010):

$$\Delta h = \lambda_{\mathrm{mix}} \frac{L}{D} \frac{V_{mix}^2}{2g} = \varphi(V_{mix}, D, L, g, \rho_{mix}, \mu_{mix}, \sigma_{mix}) \tag{10}$$

where Δh is the two-phase flow frictional pressure loss obtained by applying the Darcy–Weisbach equation, φ is a function, λ_{mix} is the mixed two-phase flow pressure loss coefficient, L is the length of the pipeline, D is the pipe diameter, V_{mix} is the mixed two-phase flow velocity, g is the gravitational acceleration, $\rho_{\mathrm{mix}} = \alpha\rho_a + (1-\alpha)\rho_w$, $\mu_{\mathrm{mix}} = \alpha\mu_a + (1-\alpha)\mu_w$, and $\sigma_{\mathrm{mix}} = \alpha\sigma_a + (1-\alpha)\sigma_w$ are the mixed two-phase flow density, dynamic viscosity, and surface tension, respectively; α is the void fraction, and subscripts a and w denote the air and water phases, respectively. On the basis of our primary analysis, applying dimensional variables leads to a lower correlation coefficient in the models in comparison with the non-dimensional ones, highlighting that using dimensional data tends to increase noises in the dataset and in the relation between the input and output variables. Therefore, the models are not able to justify the fuzzy if–then rule antecedent and consequent parameters. Furthermore, to enhance the models' applicability, developing a non-dimensional-based model can be a suitable remedy in which each variable stands for separate physical characteristics. With the use of dimensional analysis of the Buckingham Π theorem, the relevant universal non-dimensional variables governing the air-water two-phase flow pressure loss coefficient are categorized as:

$$\frac{\lambda_{mix}}{\lambda_o} = \psi(\mathrm{R}, \mathrm{F}, \mathrm{W}, C) \tag{11}$$

where $\mathrm{R} = (\rho_{\mathrm{mix}} V_{\mathrm{mix}} D)/\mu_{\mathrm{mix}}$, $\mathrm{F} = V_{\mathrm{mix}}/(gD)^{0.5}$, and $\mathrm{W} = V_{\mathrm{mix}}{}^{2}\rho_{\mathrm{mix}} D/\sigma_{\mathrm{mix}}$ are the mixed homogeneous two-phase air-water flow Reynolds number (representing the viscous force effect), Froude number (representing the gravity force effect), and Weber number (representing the surface tension force effect), respectively, and $C = \beta/(\beta+1)$ is the air concentration inside the pipeline ($\beta = W_a/W_w$, W_a, and W_w are the air and water weight inside the pipeline of the length L). Kabiri-Samani & Borghei (2010) proved that for large values of Reynolds number (R > 20,000), the relative friction factor is independent of it and thus can be dropped from the set of the dimensionless parameters. Since the minimum Reynolds number was considered as 24,000, this parameter is not a significant variable to be considered in the present non-parametric approaches. For better identification of the characteristics of two-phase flow compared with single-phase water flow, the two-phase flow frictional pressure loss coefficient λ_{mix} is normalized with the single-phase water flow pressure loss coefficient λ_o. Developing an inclusive model for evaluation of pressure loss in air-water two-phase slug flow would rely on assembling a wide range of data to involve the physical processes. Thus, the present ANN, ANN – APSO, ANFIS, and ANFIS – APSO estimator models are appraised using approximately 1,260 data points gathered by Kabiri-Samani & Borghei (2010). The statistical characteristics of the collected data applied in the present study are shown in Table 1. From the 1,260 selected data points, 880 (70%) data points were selected randomly as the training data, 250 (20%) data points as the checking data, and the remaining 130 (10%) data points were used as the testing data to evaluate the models' performances. According to this table, the ranges of the data are significantly different. For better optimization of the models, the data were normalized to be in the range of [0,1] as follows:

$$x_n = \left(\frac{x - x_{\min}}{x_{\max} - x_{\min}}\right) \Rightarrow x = x_n(x_{\max} - x_{\min}) + x_{\min} \tag{12}$$

where x, x_n, $x_{\min}$, and $x_{\max}$ are the real data, normalized data, minimum, and maximum values of data in each dataset.

Table 1 | Statistical characteristics of datasets

	Training data (Number = 880)				
	R	**F**	**W**	***C***	λ_{mix}/λ_o
Mean	60,000	1.82	634	0.43	1.16
Min.	25,000	0.10	280	0.05	0.97
Max.	100,000	5.00	950	0.85	1.34
Range	75,000	4.90	670	0.80	0.37
	Checking data (Number = 130)				
	R	**F**	**W**	***C***	λ_{mix}/λ_o
Mean	53,000	2.28	575	0.43	1.11
Min.	24,000	0.30	370	0.12	1.03
Max.	89,000	4.00	825	0.79	1.27
Range	65,000	3.70	455	0.67	0.24
	Testing data (Number = 250)				
	R	**F**	**W**	***C***	λ_{mix}/λ_o
Mean	57,000	2.70	615	0.42	1.10
Min.	29,000	0.20	290	0.12	1.01
Max.	93,000	4.80	885	0.77	1.31
Range	64,000	4.60	595	0.65	0.3

RESULTS AND DISCUSSION

The following expressions summarize the applied set of Takagi & Sugeno's (1985) fuzzy if–then rules for the estimation of normalized pressure loss coefficient of the two-phase slug flow:

$$\begin{aligned}&\text{If R is } A_1,\ \text{F is } B_1,\ \text{W is } C_1 \text{ and } C \text{ is } D_1 \text{ then } \lambda_{mix}/\lambda_o \\ &= o_1\text{R} + p_1\text{F} + q_1\text{W} + r_1 C + s_1 \\ &\text{If R is } A_2,\ \text{F is } B_2,\ \text{W is } C_2 \text{ and } C \text{ is } D_2 \text{ then } \lambda_{mix}/\lambda_o \\ &= o_2\text{R} + p_2\text{F} + q_2\text{W} + r_2 C + s_2 \\ &\text{If R is } A_i,\ \text{F is } B_i,\ \text{W is } C_i \text{ and } C \text{ is } D_i \text{ then } \lambda_{mix}/\lambda_o \\ &= o_i\text{R} + p_i\text{F} + q_i\text{W} + r_i C + s_i\end{aligned} \tag{13}$$

where A_i, B_i, C_i, and D_i are the membership functions (fuzzy values) defined for the Reynolds number, Froude number, Weber number, and concentration, respectively, which are considered as the fuzzy antecedent parameters.

Likewise, o_i, p_i, q_i, r_i, and s_i are the consequent parameters in the fuzzy if–then rules. Details of parameters for each rule of the ANFIS models are discussed in the Appendix. Accordingly, the normalized pressure loss coefficient of air-water two-phase slug flow was obtained by implementing the present ANN, ANN–APSO, ANFIS, and ANFIS–APSO models. Table 2 presents the parameters of the APSO algorithm in which the stopping criteria were met based on the number of iterations by trial-and-error procedure. Equality of the population size and the decision variables in the APSO model significantly decreases the computation load of the APSO algorithm.

Table 2 | The parameters associated with ANN–APSO and ANFIS–APSO algorithms

APSO	c_1	c_2	$iter_{max}$	w_{min}	w_{max}
ANN–APSO	0.45	0.55	500	0.42	0.89
ANFIS–APSO	0.50	0.50	100	0.40	0.90

As stated, minimizing the NRMSE of the training and checking datasets was employed as the objective function to adjust the clustering and fuzzy antecedent and consequent parameters. Table 3 represents the maximum, minimum, average and standard deviation of the error values according to the results of the developed ANN, ANN–APSO, ANFIS, and ANFIS–APSO models. The robustness of the APSO in the optimization of the ANN and ANFIS models was checked by performing 25 runs to represent their associated statistical parameters (Table 3). When the NRMSE is less than 0.01 or if the maximal iterative generations are reached, the existing algorithm training process ends.

From Table 3, we can see that the ANFIS–APSO is apparently the best among the developed models. It consumes less central processing unit (CPU) time than the others while achieving the same NRMSE. ANFIS–APSO uses the gradient descending approach to search around the P_g until the best result P_g of all the particles in the searching space does not change for 25 generations. The searching effectiveness of the algorithm was improved significantly by transitioning heuristically from the PSO to the gradient descending search. Our results indicate that ANFIS and ANFIS–APSO have roughly similar maximal recognition rates. However, ANFIS and ANFIS–APSO have a better recognition rate than the ANN and ANN–APSO models. ANFIS–APSO demonstrates more stability during the training process with less CPU time compared to the others. The best recognition rate for the ANN is 83.7%, while the best recognition rate of the ANFIS can reach around 91.5%. For ANFIS–APSO with 16 hidden nodes, the best recognition rate reaches 99.83%. As mentioned, Kabiri-Samani & Borghei (2010) found that for R >20,000 the relative friction factor is independent of Reynolds number. Since the minimum Reynolds number considered here was 24,000, this parameter is not a

Table 3 | The NRMSE for training and checking data in the proposed models

Method statistical parameters	Training error SD	Ave.	Max.	Min.	Checking error SD	Ave.	Max.	Min.
ANN	0.1127	0.096	0.117	0.074	0.1739	0.143	0.189	0.098
ANN–APSO	0.0535	0.074	0.098	0.052	0.0836	0.084	0.114	0.053
ANFIS	0.0082	0.009	0.013	0.003	0.0117	0.021	0.034	0.008
ANFIS–APSO	0.0005	0.004	0.008	0.001	0.0091	0.008	0.012	0.003

substantial variable to be taken into account in the present non-parametric approaches. Given that each input variable F, W and *C* has four membership functions and each membership function has three parameters *a*, *b* and *c*, the number of the fuzzy antecedent and consequent parameters as well as the number of fuzzy rules are 36, 256 and 64, respectively. More explanations about the membership functions and the related antecedent and consequent parameters are provided in the Appendix. Figure 6 shows the optimization process of the parameters from the best among the 25 runs. Results indicate that the APSO not only optimizes fuzzy clusters, but also prevents an overtrained model.

According to the present data analysis, ANN and ANFIS models are trapped in the local optimum while the checking and training errors are minimized. On the contrary, applying the APSO algorithm enhances the capability of the ANN and ANFIS models. This finding proves the superiority of the developed ANN–APSO and ANFIS–APSO models to the ANN and ANFIS models, respectively. We performed a sensitivity analysis to determine the most effective variables on air-water two-phase slug flow pressure loss. The influence of a variable on the estimated results precision would be evaluated by eliminating it from the model inputs. Subsequently, the estimation error is calculated. The increase in model error indicates that the removed variable is effectual; if not, it can be omitted from the analysis. The obtained error values corresponding to elimination of each variable are shown in Figure 7. According to this figure, the Froude number is the most effective variable among the others that significantly influences the two-phase slug flow pressure loss coefficient. The effects of the concentration and Weber number could not be neglected. However, for large values of Reynolds number ($R > 20{,}000$), the relative friction factor is independent of the Reynolds number (Kabiri-Samani & Borghei 2010).

To guarantee the generalization ability of the developed models and to assess performance of the models in handling a dataset that has not been yet employed in the training process, the models should also be validated using the testing data. The scatter diagrams depict the accuracy of the models comparing the observed and estimated values (Figures 8 and 9). According to these figures, the pressure loss coefficient of the two-phase slug flow is slightly greater than that of a single-phase flow. This could be attributed to the reduced water flow cross section, turbulence increase,

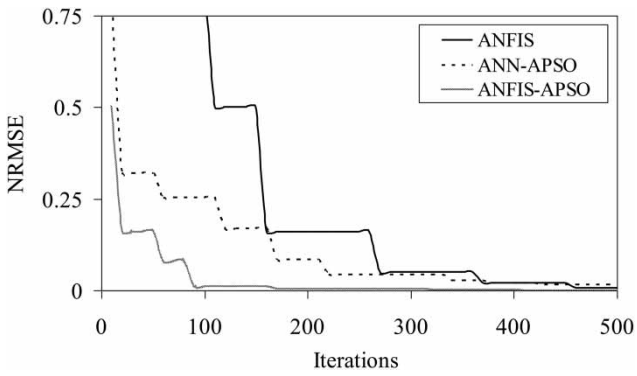

Figure 6 | Evolution of training NRMSE for different models versus the number of iterations in the estimation of air-water two-phase flow pressure loss coefficient.

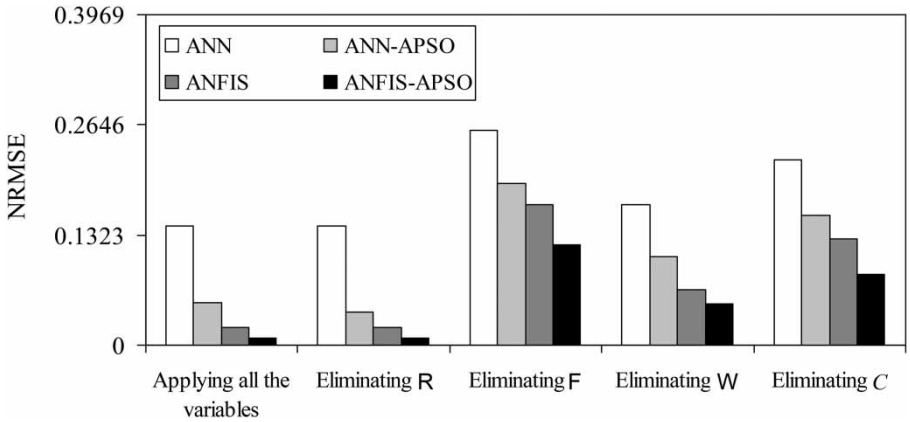

Figure 7 | Variation of training NRMSE for different models with elimination of an input variable.

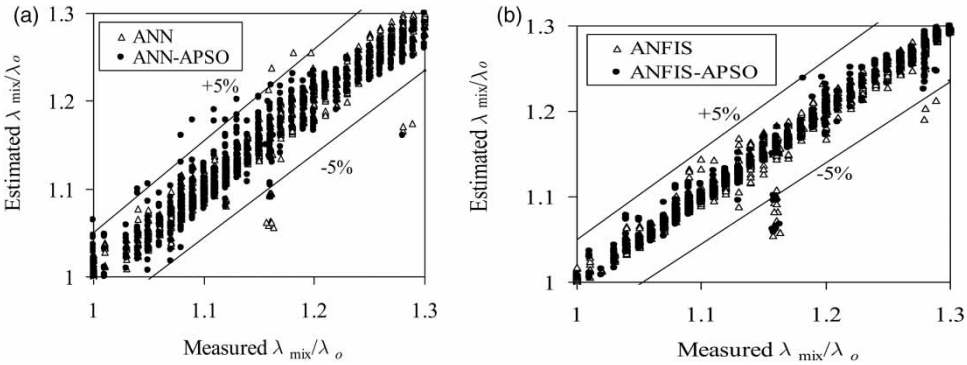

Figure 8 | Comparison estimated by (a) ANN and ANN–APSO and (b) ANFIS and ANFIS–APSO models versus measured two-phase flow normalized pressure loss coefficient associated with the training data.

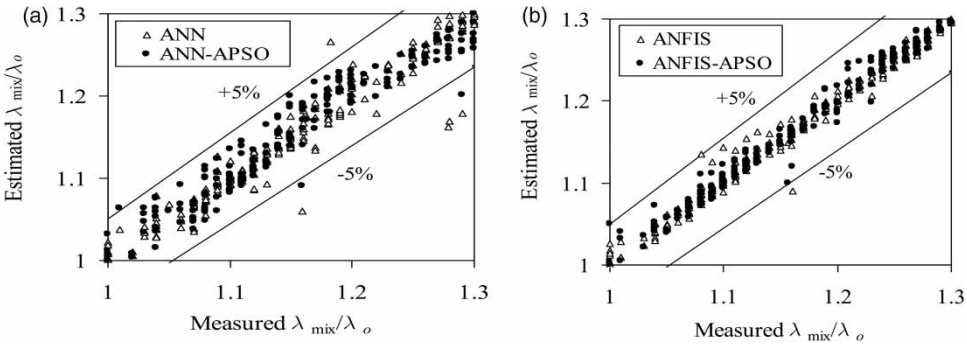

Figure 9 | Comparison estimated by (a) ANN and ANN–APSO and (b) ANFIS and ANFIS–APSO models versus measured two-phase flow normalized pressure loss coefficient associated with the testing data.

bubble generation inside the pipe, and irregular interface between the two phases. These phenomena induce a complex flow with increasing friction pressure losses coefficient. The results of statistical analysis including bias, SE and R^2 (Zanganeh *et al.* 2011) for estimation of two-phase flow pressure loss coefficient via the ANN, ANN–APSO, ANFIS, and ANFIS–APSO models and available empirical models are shown in Table 4. As can be seen, the combined ANFIS–APSO model has the greatest accuracy followed by ANFIS, ANN–APSO, and ANN. All the above mentioned models overestimate the two-phase flow pressure loss coefficient. However, the ANFIS–APSO model estimates two-phase slug flow pressure loss coefficient with a satisfactory accuracy (bias = 0.034, SE% = 8.45 and $R^2 = 0.989$). The empirical methods of Lockhart & Martinelli (1949), Muller & Heck (1986), Mishima & Hibiki (1996), Lee & Lee (2001) and Kabiri-Samani & Borghei (2010) obviously underestimate the two-phase flow pressure loss coefficient, whereas the empirical correlation presented in Zhang *et al.* (2010) overestimates the two-phase flow pressure loss coefficient. The above results indicate that ANFIS–APSO performs better than the other

Table 4 | The results of statistical analysis for the estimation of two-phase flow pressure loss coefficient

Method	SE%	bias	R^2
ANN	36.49	0.174	0.873
ANN-APSO	23.71	0.118	0.919
ANFIS	14.73	0.084	0.943
ANFIS-APSO	8.45	0.034	0.989
Equation (14)	10.12	0.063	0.961
Kabiri-Samani & Borghei (2010)	17.56	–0.113	0.947
Zhang *et al.* (2010)	18.22	0.211	0.931
Lee & Lee (2001)	21.14	–0.317	0.725
Mishima & Hibiki (1996)	29.71	–5.236	0.629
Muller & Heck (1986)	35.43	–11.76	0.324
Lockhart & Martinelli (1949)	48.96	–23.77	0.261

models in noisy media of air-water two-phase flow phenomenon.

Running the best ANFIS-APSO model for an extensive set of random values of independent variables (e.g. F, W and C), a wide range of data (about 4,500 data for $F \leq 1$ and 5,000 data for $F > 1$) was obtained for λ_{mix}/λ_o. All the measured and estimated datasets applying the ANFIS-APSO were used to derive a general expression for prediction of air-water two-phase slug flow pressure loss coefficient for both $F \leq 1$ and $F > 1$. By implementing a non-linear regression analysis using the SPSS mathematical software and through a trial and error procedure, the best equation fit to the data points, with the most accurate results, was obtained as:

$$\frac{\lambda_{mix}}{\lambda_o} = -0.15F^{-1.10}W^{-0.33} + 0.31F^{-0.33}C^{0.31} + 0.97 \qquad (14)$$

subject to the present tests limitations, i.e. $0.1 \leq F \leq 5.0$, $280 \leq W \leq 1{,}000$, $0.1 \leq C \leq 0.8$. According to the sensitivity and error analyses, Equation (14) can be used by design engineers to predict the pressure loss in air-water two-phase slug flow problems even by invoking other databases with acceptable precision (Table 4). Investigating a lot of measured and predicted data, Equation (14) can predict pressure loss in air-water two-phase slug flow more accurately than the traditional equations in the literature (Lockhart & Martinelli 1949; Muller & Heck 1986; Mishima & Hibiki 1996; Lee & Lee 2001; Kabiri-Samani & Borghei 2010; Zhang *et al.* 2010). Notwithstanding the lower accuracy of Equation (14) relative to the ANFIS-APSO model, it can be easily used by the hydraulic and environmental engineers in various design problems.

SENSITIVITY ANALYSIS AND PHYSICAL MEANING OF THE RESULTS

Applying the StatSoft method, a sensitivity analysis was performed to investigate the sensitivity of model to its input variables. The StatSoft method calculates the sensitivity coefficient for an input variable, divided by the total error of the model, excluding such a variable in the presence of all the other input variables. While the sensitivity coefficient of a variable is more than unity, such a variable has a great contribution to the variability of the output component, e.g. the pressure loss coefficient (Table 5). Accordingly, the average air concentration has the greatest effect on pressure loss coefficient compared to the other effective dimensionless input variables. Reducing water flow cross section, increasing flow, generating bubbles around the pipe wall and establishing regular-irregular flow interface between the two phases results in a complex flow behavior with $\lambda_{mix} > \lambda_o$ or perhaps $\lambda_{mix} < \lambda_o$. By increasing the Weber number, for a given concentration, λ_{mix}/λ_o increases. However, according to Table 5, among F, W and C, the Weber number W has the least effect on the variation of pressure loss coefficient. Since the flow was fully turbulent with $R > 20{,}000$, the viscous effect was minimum and the Reynolds number, R, can be excluded from the dimensionless prevailing parameters. Considering these criteria, it can be inferred that the scale effects were minimal in the present study.

Table 5 | Results of sensitivity analysis for the input variables to predict the pressure loss coefficient

Input variables	Removed variable	MSE	Sensitivity coefficient
F, W, C	–	0.0019	–
W, C	F	0.0095	5
F, C	W	0.0025	1.31
W, F	C	0.084	44.21

CONCLUDING REMARKS

In this paper we applied a hybrid APSO algorithm combined with ANN and ANFIS models. The APSO benefits from the capabilities of the PSO and BP algorithms in global and local search, respectively. In the developed hybrid algorithms, the early particles are distributed randomly in the searching space and then a global search is performed around the global optimum.

The study makes use of heuristic knowledge to transfer the APSO algorithm to the gradient descending searching until the best fitness value in the history of all particles became constant for some generations. The effective dimensionless parameters were found with less clustering radii than the other ones. Furthermore, the application of

dimensional models exerts noises on the system so that the present models are not capable of adjusting the fuzzy if–then rule parameters. Hence, the non-dimensional-based models were developed based on dimensional analysis. Results of the sensitivity analysis indicated that the mixed homogeneous two-phase flow Froude and Weber numbers and the air concentration are the most significant variables to affect the two-phase flow normalized pressure loss coefficient. Considering the available criteria in the literature, the viscosity effect is negligible if the Reynolds numbers $R > 20{,}000$. Satisfying this criterion, thereby minimizing the effect of viscosity on the pressure loss coefficient, R was diminished from the set of effective dimensionless parameters.

Our findings show that the ANFIS–APSO algorithm consumes less CPU time to achieve a higher training accuracy than the other algorithms. The best agreement was achieved between the measured and the predicted values using the ANFIS-APSO model, indicating that this model is more convenient and could predict the frictional pressure loss with reasonable accuracy. Results show that the ANFIS-APSO model is superior to the other developed models in terms of convergence speed and accuracy. It outperforms the existing methods and published correlations and shows promising capabilities in solving different air-water two-phase flow problems. According to the results, the ANFIS-APSO model performs better than the empirical correlations in the literature. Equation (14), obtained based on an extensive set of measured data and model predictions, offers a simple and applicable relation for design purposes.

Finally, the proposed model offers a practical means for the prediction of pressure loss in air-water two-phase slug flow design problems, even by applying other databases with acceptable precision. Although we endeavored to meet standard conditions for producing the database and generalizing the developed models, researchers and design engineers are cordially invited to share their databases and developed models to improve the present model.

ACKNOWLEDGEMENTS

The authors gratefully acknowledge the generous assistance and constructive comments of Dr Milad Aminzadeh, Isfahan University of Technology, Iran.

DATA AVAILABILITY STATEMENT

The data will be added to the home page of the core author at: kabiri.iut.ac.ir

REFERENCES

Autee, A. T. & Giri, S. V. 2016 Experimental study on two-phase flow pressure drop in small diameter bends. *Perspect. Sci.* **8**, 621–625. doi:10.1016/j. pisc.2016.06.038.

Azamathulla, H. M. & Ahmad, Z. 2013 Estimation of critical velocity for slurry transport through pipeline using adaptive neuro-fuzzy interference system and gene-expression programming. *J. Pipeline Sys. Eng. Prac.* **4** (2), 131–137. doi:10.1061/(ASCE)PS.1949-1204.0000123.

Bara, N., Dasa, S. K. & Biswasb, M. N. 2013 Prediction of frictional pressure drop using artificial neural network for air-water flow through U-bends. *Procedia Tech.* **10**, 813–821. doi:10.1016/j.protcy.2013.12.426.

Carlisle, A. & Dozier, G. 2001 An off-the-shelf APSO. In *Proc. Particle Swarm Opt. Workshop*. Purdue School of Engineering and Techology, Indianapolis, pp. 1–6.

Chen, J.-C., Shu, C.-S., Ning, S.-K. & Chen, H.-W. 2008 Flooding probability of urban area estimated by decision tree and artificial neural networks. *J. Hydroinform.* **10** (1), 57–67. doi:10.2166/hydro.2008.009.

Chisholm, D. 1967 A theoretical basis for the Lockhart-Martinelli correlation for two-phase flow. *Int. J. Heat Mass Transfer.* **10** (12), 1767–1778. doi:10.1016/0017-9310(67)90047-6.

Chiu, S. 1994 Fuzzy model identification based on cluster estimation. *J. Intelli. Fuzzy Sys.* **2**, 267–278. doi:10.3233/IFS-1994-2306.

Dang, Z., Yang, Z., Yang, X. & Ishii, M. 2019 Experimental study on void fraction, pressure drop and flow regime analysis in a large ID piping system. *Int. J. Multiphase Flow.* **111**, 31–41. doi:10.1016/j.ijmultiphaseflow.2018.10.006.

Ehteram, M., Mousavi, S. F., Karami, H., Farzin, S. & Singh, V. P. 2018 Reservoir operation based on evolutionary algorithms and multi-criteria decision-making under climate change and uncertainty. *J. Hydroinform.* **20** (2), 332–355. doi:10.2166/hydro.2018.094.

Eyhavand-Koohzadi, A., Borghei, S. M. & Kabiri-Samani, A. R. 2016 Water hammer in a horizontal rectangular conduit containing air-water two-phase slug flow. *J. Hydraul. Eng.* **142** (3), 1–10. doi:10.1061/(ASCE)HY.1943-7900.0001098.

Hanbay, D., Baylar, A. & Ozpolat, E. 2009 Predicting flow conditions over stepped chutes based on ANFIS. *Soft Comput.* **13**, 701–707. doi:10.1007/s00500-008-0343-7.

Jang, J. S. R. 1993 Adaptive-network-based fuzzy inference systems. *IEEE Trans. Sys. Man Cybern.* **23** (3), 665–685. doi:10.1109/21.256541.

Kabiri-Samani, A. R. & Borghei, S. M. 2010 Pressure loss in a horizontal two-phase slug flow. *J. Fluids Eng.* **132** (7), 1–8. doi:10.1115/1.4001969.

Kabiri-Samani, A. R., Borghei, S. M. & Saidi, M. H. 2007 Fluctuation of air-water two-phase flow in horizontal and inclined water pipelines. *J. Fluids Eng.* **129** (1), 1–14. doi:10.1115/1.2375134.

Kabiri-Samani, A. R., Aghaee-Tarazjani, J., Borghei, S. M. & Jeng, D. S. 2011 Application of neural networks and fuzzy logic models to long-shore sediment transport. *App. Soft Comp.* **11** (2), 2880–2887. doi:10.1016/j.asoc.2010.11.021.

Kennedy, J. & Eberhart, R. C. 1995 Particle swarm optimization. In *Proc. of IEEE Int. Conf. Neural Network*, Perth, Australia. IEEE Service Center, Piscataway, NJ, USA, pp. 1942–1948.

Kong, R., Kim, S., Bajorek, S., Tien, K. & Hoxie, C. 2018 Effects of pipe size on horizontal two-phase flow: flow regimes, pressure drop, two-phase flow parameters, and drift-flux analysis. *Exp. Therm. Fluid Sci.* **96**, 75–89. doi:10.1016/j.expthermflusci.2018.02.030.

Lavin, F. L., Kanizawa, F. T. & Ribatski, G. 2019 Analyses of the effects of channel inclination and rotation on two-phase flow characteristics and pressure drop in a rectangular channel. *Exp. Therm. Fluid Sci.* **109**, 109850. doi:10.1016/j.expthermflusci.2019.109850.

Le Corre, J. M., Aldorwish, Y., Kim, S. & Ishi, M. 1999 Two-phase flow pattern identification using a fuzzy methodology. In *Proceedings 1999 International Conference on Information Intelligence and Systems*. IEEE Service Center, Bethesda, MD, USA, pp. 155–161, doi:10.1109/ICIIS.1999.810248.

Lee, H. & Lee, S. 2001 Pressure drop correlations for two-phase flow within horizontal rectangular channels with small heights. *Int. J. Mltiphase Flow.* **27** (5), 783–796. doi:10.1016/S0301-9322(00)00050-1.

Leonardis, A. & Bischof, H. 1998 An efficient MDL-based construction of RBF networks. *Neural Netw.* **11**, 963–973. doi:10.1016/S0893-6080(98)00051-3.

Lewis, J. M. & Wang, Y. 2019 Two phase frictional pressure drop in a thin mixed-wettability microchannel. *Int. J. Heat Mass Transf.* **128**, 649–667. doi:10.1016/j.ijheatmasstransfer.2018.09.010.

Lima, G. M., Brentan, B. M., Manzi, D. & Luvizotto, E. 2017 Metamodel for nodal pressure estimation at near real-time in water distribution systems using artificial neural networks. *J. Hydroinform.* **20** (2), 486–496. doi:10.2166/hydro.2017.036.

Lockhart, R. W. & Martinelli, R. C. 1949 Proposed correlation of data for isothermal two-phase, two-component flow in pipes. *Chem. Eng. Prog.* **45** (1), 39–48.

Mahvash, A. & Ross, A. 2008 Application of CHMMs to two-phase flow pattern identification. *Eng. Appl. Artif. Intell.* **21** (8), 1144–1152. doi:10.1016/j.engappai.2008.02.005.

Mandhan, J. M., Gregory, G. A. & Aziz, K. 1974 A flow pattern map for gas-liquid flow in horizontal pipes. *Int. J. Multiphase Flow* **1**, 537–553.

MathWorks, R2007b. 2007 *Matlab and Simulink Neural Networks/Fuzzy Logic Toolbox*. The MathsWorks Inc., Natick, MA, USA.

McClymont, K., Keedwell, E. C., Savić, D. & Randall-Smith, M. 2013 Automated construction of evolutionary algorithm operators for the bi-objective water distribution network design problem using a genetic programming based hyper-heuristic approach. *J. Hydroinform.* **16** (2), 302–318. doi:10.2166/hydro.2013.226.

Mi, Y., Ishii, M. & Tsoukalas, L. H. 1998 Vertical two-phase flow identification with advanced instrumentation and neural networks. *Nucl. Eng. Des.* **184**, 409–420. doi:10.1016/S0029-5493(98)00212-X.

Mishima, K. & Hibiki, T. 1996 Some characteristics of air-water two-phase flow in small diameter vertical tubes. *Int. J. Multiphase Flow* **22** (4), 703–712. doi:10.1016/0301-9322(96)00010-9.

Mousavi, S. J. & Shourian, M. 2009 Capacity optimization of hydropower storage projects using particle swarm optimization algorithm. *J. Hydroinform.* **12** (3), 275–291. doi:10.2166/hydro.2009.039.

Muleta, M. K. & Nicklow, J. W. 2002 Evolutionary algorithms for multiobjective evaluation of watershed management decisions. *J. Hydroinform.* **4** (2), 83–97. doi:10.2166/hydro.2002.0010.

Muller, H. & Heck, K. 1986 A simple friction pressure drop correlation for two-phase flow in pipes. *Chem. Eng. Process.* **20** (6), 297–308. doi:10.1016/0255-2701(86)80008-3.

Najafzadeh, M. 2019 Evaluation of conjugate depths of hydraulic jump in circular pipes using evolutionary computing. *Soft Comput.* **23**, 13375–13391. doi:10.1007/s00500-019-03877-9.

Najafzadeh, M. & Bonakdari, H. 2017 Application of a neuro-fuzzy GMDH model for predicting the velocity at limit of deposition in storm sewers. *J. Pipeline Syst. Eng. Pract.* **8** (1), 13375–13391. doi:10.1061/(ASCE)ps.1949-1204.0000249.

Najafzadeh, M. & Saberi-Movahed, F. 2016 GMDH-GEP to predict free span expansion rates below pipelines under waves. *Mar. Georesour. Geotechnol.* **37** (3), 375–392. doi:10.1080/1064119X.2018.1443355.

Najafzadeh, M. & Sattar, M. A. 2015 Neuro-fuzzy GMDH approach to predict longitudinal dispersion in water networks. *Water Resour. Manage.* **8**, 2205–2219. doi:10.1007/ s11269-015-0936-8.

Najafzadeh, M. & Shahid, A. E. 2016 Scour prediction in long contractions using ANFIS and SVM. *Ocean Eng.* **111**, 128–135. doi:10.1016/j.oceaneng.2015.10.053.

Roshani, G. H., Karami, A. & Nazemi, E. 2018 Combination of a gamma radiation-based system and the adaptive network-based fuzzy inference system (ANFIS) for calculating the volume fraction in stratified regime of a three-phase flow. *Radiat. Detect. Tech. Methods* **2** (38), 1–13. doi:10.1007/s41605-018-0053-3.

Rumelhart, D. E., Hinton, G. E. & Williams, R. J. 1986 Learning representations by back-propagating errors. *Nature* **323**, 533–536.

Saberi-Movahed, F., Najafzadeh, M. & Mehrpooya, A. 2020 Receiving more accurate predictions for longitudinal dispersion coefficients in water pipelines: training group method of data handling using extreme learning machine conceptions. *Water Resour. Manage.* **34**, 529–561. doi:10.1007/s11269-019-02463-w.

Seckin, N. 2010 Modeling flood discharge at ungauged sites across Turkey using neuro-fuzzy and neural networks. *J. Hydroinform.* **13** (4), 842–849. doi:10.2166/hydro.2010.046.

Shi, Y. & Eberhart, R. C. 1998 A modified particle swarm optimizer. *Proc. IEEE World Conf. Compu. Intelli.* 69–73. doi:10.1109/ICEC.1998.699146.

Shokouh Saljoughi, A., Mehvarz, M. & Mirvaziri, H. 2017 Attacks and intrusion detection in cloud computing using neural networks and particle swarm optimization algorithms. *Emerg. Sci. J.* **1** (4), 179–194. doi:10.28991/ijse-01120.

Sinha, N. K., Gupta, M. M. & Zadeh, L. A. 2000 *Soft Computing and Intelligent Systems: Theory and Applications*. Academic Press, London, UK.

Sunde, C., Avdic, S. & Pázsit, I. 2005 Classification of two-phase flow regimes via image analysis and a neuro-wavelet approach. *Prog. Nucl. Energy* **46**, 348–355. doi:10.1016/j.pnucene.2005.03.015.

Takagi, T. & Sugeno, M. 1985 Fuzzy identification of systems and its applications to modeling and control. *IEEE Trans. Sys. Man Cybern.* **15**, 116–132. doi:10.1109/TSMC.1985.6313399.

Thomas, A., Eldho, T. I., Rastogi, A. K. & Majumder, P. 2019 A comparative study in aquifer parameter estimation using MFree point collocation method with evolutionary algorithms. *J. Hydroinform.* **21** (3), 455–473. doi:10.2166/hydro.2019.105.

Timung, S. & Mandal, T. K. 2013 Prediction of flow pattern of gas–liquid flow through circular microchannel using probabilistic neural network. *App. Soft Comp.* **13** (4), 1674–1685. doi:10.1016/j.asoc.2013.01.011.

Tsoukalas, L. H., Ishii, M. & Mi, Y. 1997 A neuro-fuzzy methodology for impedance-based multiphase flow identification. *Eng. Appl. Artif. Intell.* **10**, 545–555. doi:10.1016/S0952-1976(97)00037-7.

Woods, B. D., Fan, Z. & Hanratty, T. J. 2006 Frequency and development of slugs in a horizontal pipe at large liquid flows. *Int. J. Multiphase Flow* **32** (8), 902–925. doi:10.1116/j.ijmultiphaseflow.2006.02.020.

Zanganeh, M., Yeganeh-Bakhtiary, A. & Bakhtyar, R. 2011 Combined particle swarm optimization and fuzzy inference system model for estimation of current-induced scour beneath marine pipelines. *J. Hydroinform.* **13** (3), 558–573. doi:10.2166/hydro.2010.101.

Zhang, Z., Li, C.-W., Li, Y.-S. & Qi, Y. 2006 Incorporation of artificial neural networks and data assimilation techniques into a third-generation wind–wave model for wave forecasting. *J. Hydroinform.* **8** (1), 65–76. doi:10.2166/jh.2006.005.

Zhang, W., Hibiki, T. & Mishima, K. 2010 Correlations of two-phase frictional pressure drop and void fraction in mini channel. *Int. J. Heat Mass.* **53** (1–3), 453–465. doi:10.1016/j.ijheatmasstransfer.2009.09.011.

First received 5 June 2020; accepted in revised form 2 October 2020. Available online 6 November 2020